Microscopy and Spectroscopy of Interactions between Metallopolymers and Carbon Nanotubes

Fiona Frehill,[†] Marc in het Panhuis,*[,‡] Nigel A. Young,[‡] William Henry,[†] Johan Hjelm,[†] and Johannes G. Vos[†]

National Centre for Sensor Research, School of Chemical Sciences, Dublin City University, Dublin 9, Ireland, and Department of Chemistry, The University of Hull, Hull, HU6 7RX, United Kingdom

Received: March 21, 2005; In Final Form: May 24, 2005

The interaction between redox polymers, based on Ru- or Os-bis(2,2′-bipyridyl)-poly(4-vinylpyridine), and carbon nanotubes was investigated by spectroscopic and microscopic techniques. These metallopolymers were found to be excellent dispersants for nanotubes, as a result of a good wetting interaction between polymer and nanotubes. The results obtained show that well-coated individual nanotubes can be obtained. In addition, interactions between nanotubes and polymers did not significantly affect the electronic and electrochemical properties of the metallopolymers. On the basis of the electrochemical properties of the polymers this opens the possibility of adding functionality through interaction with nanotubes, either as redox active materials with enhanced mechanical properties or by using these modified nanotubes as nanosized electrochemical sensors.

1. Introduction

Since their discovery in 1991[1] carbon nanotubes have attracted considerable attention, mainly because their unique combination of mechanical, thermal, optical, and electrical properties may form the basis of many potential applications.[2−4] However, processing and manipulation of carbon nanotubes is limited by their lack of solubility in most solvents. Therefore, successful incorporation of nanotubes into materials requires the development of methods for their effective dispersion. Decreasing nanotube aggregation in solution and improving solubility are areas of intensive research. Compounds such as saccharides,[5,6] surfactants,[7−10] ceramics,[11] biological entities,[12,13] synthetic polymers,[14−25] and chemically modified soy oil[26] have been used to disperse single-walled (SWNT) and multiwalled (MWNT) carbon nanotubes through noncovalent functionalization. Polymers are attractive materials since they may be easily processed and fabricated into solid-state forms such as thin films required in most applications.[27] In addition to acting as efficient nanotube dispersing agents, employing polymers in composites is of interest because they allow for a novel combination of nanotube and polymer properties. Previous work established that the formation of stable polymer−nanotube composites depends on a good wetting interaction between polymers and nanotubes.[14,16] This in turn has been found to be dependent in particular on the polymer chain conformation.[16,19] In addition it was determined that certain polymers form crystalline layers around nanotubes thereby increasing polymer backbone−nanotubes interactions.[23,24]

Composite materials from nanotubes and conducting polymers have been investigated.[19,21,22,25] The electrochemical activity in these polymers is based on the electronic and electrochemical properties of the polymer backbone. On the other hand, for redox polymers such as materials of the type $[M(bpy)_2(PVP)_{10}Cl]Cl$ (see Figure 1), where M = Ru or Os, bpy is 2,2′-bipyridine, and PVP is poly(4-vinyl)pyridine, considered in this paper, the electrochemically active moieties are not related to the backbone but are based on pendent groups of the type $M(bpy)_2-$, which are covalently linked to the polymer backbone.[28−30] The polymers are of interest since their electrochemistry is extremely reversible and the materials are very stable in several oxidation states. They have therefore been used extensively as redox catalysts for the sensing of analytes such as Fe(II)/Fe(III), nitrite, and ascorbic acid and have been applied in biosensor assemblies.[31−35] In addition, there is a well-developed synthetic chemistry for these redox metallopolymers containing poly(pyridyl) complexes of ruthenium(II) and osmium(II) and their redox potential can be varied systematically.[36]

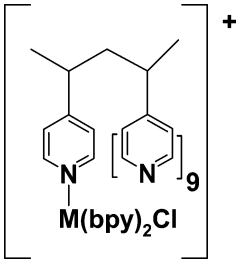

Figure 1. Structure of metallopolymers $[M(bpy)_2PVP_{10}Cl]Cl$, with M = Ru or Os.

In this contribution, (noncovalent) interactions between two redox metallopolymers and single-walled and multiwalled carbon nanotubes are investigated, using a range of microscopic and spectroscopic techniques.

2. Experimental Details

SWNT[37] were prepared by high-pressure decomposition of carbon monoxide (HiPco) obtained from Carbon Nanotechnologies, Inc. (Houston, USA, batch no. P0-185). Catalytic chemical vapor deposition (CVD) produced MWNT were

* To whom correspondence should be addressed. E-mail: M.Panhuis@hull.ac.uk.
[†] Dublin City University.
[‡] The University of Hull.

10.1021/jp051459o CCC: $30.25
Published on Web 06/18/2005

obtained from Nanocyl S.A. (Belgium, batch no. NFL60). The metallopolymers $[Ru(bpy)_2PVP_{10}Cl]Cl$ and $[Os(bpy)_2PVP_{10}Cl]Cl$ where bpy is 2,2′-bipyridine and PVP is poly(4-vinyl)pyridine were prepared as described previously.[36]

Nanotube dispersions were prepared by sonicating SWNT or MWNT in a 0.5% (weight per volume) methanolic solution of the polymer until a dense black dispersion had formed. The resulting composites are the following: $[Ru(bpy)_2PVP_{10}Cl]Cl-$MWNT **1**, $[Ru(bpy)_2PVP_{10}Cl]Cl-$SWNT **2**, $[Os(bpy)_2PVP_{10}Cl]Cl-$MWNT **3**, and $[Os(bpy)_2PVP_{10}Cl]Cl-$SWNT **4**.

UV−vis absorption spectra (accuracy ±2 nm) were recorded in 10 mm quartz cuvettes on a Shimadzu UV−vis−NIR 3100 spectrophotometer interfaced with an Elonex PC466, using a UV−vis data manager. Raman spectra were collected in 180° scattering geometry with a Bruker FRA 106/S Raman module mounted on a Bruker Equinox55 FTIR bench with a cw Nd:YAG 1064 nm laser at ca. 100 mW, a CaF_2 beam splitter, and a liquid nitrogen cooled Ge detector. Transmission electron microscopy (TEM) images were obtained on a JEOL 2011 TEM. Diluted composite solutions were evaporated onto Cu 300 mesh grids. Tapping mode atomic force microscopy (TM-AFM) was carried out in an air environment with use of a Digital Instruments Nanoscope IIIa. Laser alignment was performed manually, and cantilever tuning and drive frequency selection was automatically performed by the DI software. The cantilevers used are made of silicon and have a triangular pyramid shape, a tip radius <10 nm, a force constant of 25−60 N/m, and a resonant frequency of 150−190 kHz. The carbon nanotube polymer composites for TM-AFM analysis were prepared on native oxide-covered Si(111) substrates. Initially a SiO_2 wafer was cleaned by sonication in acetone and ethanol for 5 min each, and then gently boiled in piranha solution (H_2O_2:NH_4:H_2O (1:1:5)) for 25 min (to remove any form of organic contaminants and trace metals). The wafers were rinsed with Milli-Q water and dried under argon. A 1% (v/v in Milli-Q water) solution of 3-(aminopropyl)triethoxysilane (APS, Aldrich) was dropped onto a cleaned wafer and allowed to react for up to 10 min. The wafers were rinsed with Milli-Q water and dried under argon. The various carbon nanotube polymer composite solutions (in methanol) were drop-cast onto the silanized wafer. In one set of samples the silanized wafers coated with the polymer solution were allowed to stand for 10 min. The wafers were then rinsed with Milli-Q water and dried under argon after which TM-AFM analysis was carried out. In the second set of samples no washing with water was carried out and the polymer-coated surfaces were allowed to stand for 24 h until the methanol evaporated and subsequently TM-AFM analysis was carried out.

3. Results and Discussion

Absorption spectroscopy has proved useful in the characterization of ruthenium- and osmium-based polymers[36,38] and to examine the effects of interaction with nanotubes on polymers.[15,16] UV−visible absorption spectra for the $[Ru(bpy)_2PVP_{10}Cl]Cl$ polymer and its polymer−nanotube composites are shown in Figure S1 in the Supporting Information (composite **1**) and Figure 2 (composite **2**). The spectrum for the Ru-metallopolymer is dominated by two characteristic bands at 350 and 498 nm attributed to a single metal-to-ligand charge-transfer (^{1}MLCT) transition. The analogous osmium metallopolymer exhibits similar MLCT bands at 364 and 481 nm and an additional broad feature with a maximum at about 700 nm (see Figure S2 in the Supporting Information). The latter has been assigned to a spin-forbidden ^{3}MLCT transition, which is partly allowed by the considerable spin−orbit coupling present in the Os metal ion.[36]

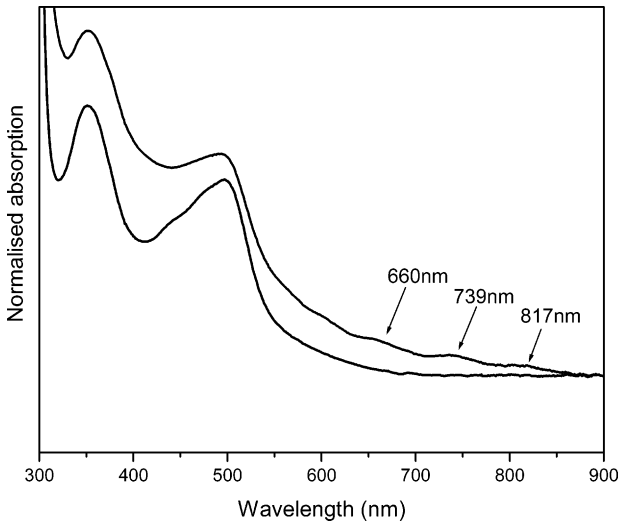

Figure 2. UV−visible absorption spectra of $[Ru(bpy)_2PVP_{10}Cl]Cl$ (top line), and composite **2** (bottom line, SWNT) normalized to 900 nm.

In comparison to the metallopolymers no significant changes are observed in the positions of the spectroscopic features for the composite materials. However, the relative intensity of the band associated with MCLT transitions is significantly reduced in the composite material. In addition, broad features at 660, 739, and 817 nm in the absorption spectrum of composite **2** (see Figure 2) confirm the presence of nanotubes. These bands can be attributed to transitions between van Hove singularities in SWNT aggregates similar to our previous observations.[19] The UV−vis spectral features indicate that the overall structure of the metallopolymers is not significantly changed. This is confirmed by electrochemical studies (not shown), which show that the redox potentials of the composites are very close to those observed for the polymers themselves. The spectroscopic data do, however, indicate the presence of both carbon nanotubes and polymer.

Raman spectroscopy is a spectroscopic tool used to probe carbon nanotubes in polymer composites and can provide insight into the interaction between polymer and nanotubes.[18,19] Raman spectra of HiPco SWNT have been extensively studied and are well understood.[39] Figure S3 (in the Supporting Information) shows the room-temperature Raman spectra of HiPco SWNT and composite **2** for laser excitation at 1064 nm (1.17 eV). The observed features for SWNT are assigned as follows: low-frequency radial breading modes (RBM, below 400 cm^{-1}), the disorder induced D band (around 1275 cm^{-1}), tangential C−C stretching mode features (G bands, near 1590 cm^{-1}), and two-phonon-scattering processes (between 1600 and 3000 cm^{-1}).[39] It has been noted that the various modes in the range 500−1200 cm^{-1} are only observed for this particular excitation wavelength and were attributed to enhancement of Raman cross-section for small-diameter (below 1.0 nm) SWNT.[39] Carbon nanotube features dominate the Raman spectrum of the composite (Figure S3, black line). The intertube interaction in SWNT bundles is dominated by van der Waals interactions. It is well-known that noncovalent sidewall functionalization of nanotubes results in an upshift of the radial breathing modes features.[6,12,15,18,19,26] The magnitude of the upshift depends on the degree of (partial) intercalation of the dispersant between nanotubes in bundles and coating of bundles. In comparison with the HiPco spectrum, the upshifts for the composite are as follows: RBM features by up to 4 cm^{-1}, D-band by 5.8 cm^{-1}, and G-bands by 2.1 cm^{-1}. Therefore, the observed shifts in nanotube features suggest that the Ru-metallopolymer interacts

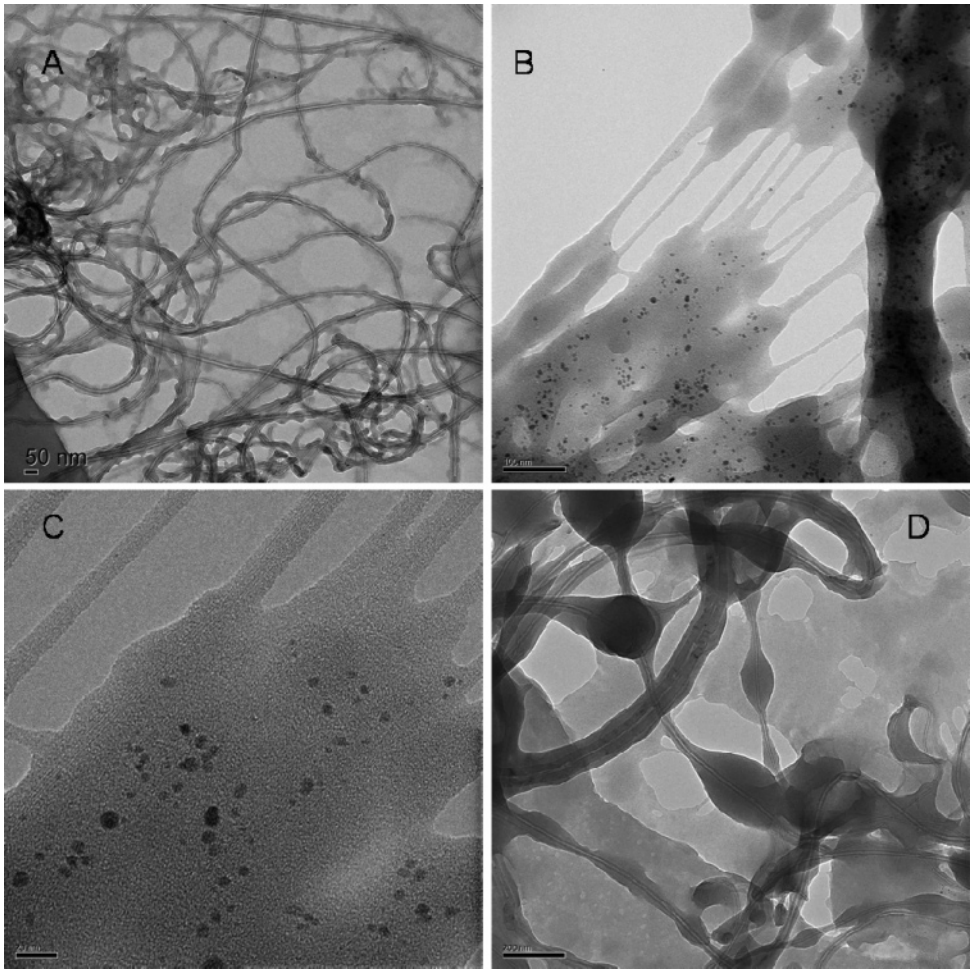

Figure 3. Transmission electron microscopy (TEM) images: (A) Low-resolution images of composite **1** showing wetting of MWNT by Ru-metallopolymers (scale bar 50 nm). (B) Low-resolution image of composite **2** (scale bar 100 nm) and (C) high-resolution image of composite **2** (scale bar 20 nm) showing bundles of SWNT wetted by the Ru-metallopolymer. Dark spheres are Fe catalyst particles used in HiPco synthesis. (D) Low-resolution images of composites **3** showing wetting of MWNT by Os-metallopolymers (scale bar 200 nm).

with nanotubes. Similar observations were made for the other composites (not shown).

Electron microscopy is an excellent technique for investigating the wetting between polymers and nanotubes as both can be readily identified in the images. Figure 3 shows TEM images of composites **1**−**3**. The nanotubes are visible as the darker thin lines, with the hollow core of the nanotube visible within. Nanotubes produced by CVD (Figure 3A,D) and HiPco (Figure 3B,C) techniques are structurally different as is evident from the images. CVD-produced tubes contain structural defects resulting in bends in the nanotube bodies. HiPco tubes contain fewer defects and therefore appear as mainly straight lines. In addition, as CVD tubes are MWNT (consisting of multiple carbon shells) they are thicker and longer compared to the SWNT (consisting of a single carbon shell) produced by the HiPco process. It is evident from the images that both types of nanotubes are nicely and completely covered by metallopolymer. In particular, composites **1** and **3** consist of individual MWNT coated by a thick layer of polymer. Whereas in composites **2** and **4** (not shown**)**, SWNT appear in bundles (or aggregates) coated in polymer. This is indicative of good binding as the nanotubes support a large amount of polymer.

TM-AFM was used to investigate the difference in surface topography between MWNT and polymer−nanotube composites. Height analysis of unmodified MWNT (Figure S4 in the Supporting Information) suggests a nanotube thickness of 50−60 nm, in good agreement with the manufacturer's specification. Height analysis with AFM is only approximate due to surface interactions and flattening of the tube on the surface. Images of composite **1** drop-cast from solution on a wafer can be observed in Figure 4. Ru-metallopolymer covered MWNT (straight lines) and free polymer (spherical objects) can be clearly identified. Subsequently, a sample of composite **1** was prepared by allowing the composite solution to react with the amino-functionalized surface for 10 min, after which the substrate was washed with a small quantity of Milli-Q water. The resulting images (Figure 5) show that the nanotubes are noncovalently bound to the surface whereas free polymer (evidently present in Figure 4) is washed from the substrate. This allows for more reliable height analysis. $[Ru(bpy)_2PVP_{10}Cl]Cl$ does not readily dissolve in water but may be removed from the surface as the methanolic solution has not evaporated. Thus aggregates of composite **1** are now readily identified (in Figure 5), without the presence of excess polymer. Height analysis suggests a thickness of 165−200 nm for the polymer-coated MWNT. Similar observations may be made for the polymer−tube composites **2**, **3**, and **4** (see Figures S5−S7 in the Supporting Information). This coating method incorporating a washing cycle provides a technique for forming aggregates of polymer−nanotube composites without the presence of free polymer.

In previous studies on polymers such as poly(*p*-phenylene vinylene-*co*-2,5-dioctyloxy-*m*-phenelyne-vinylene) (PmPV)[16,40] and electroactive polyaniline[19] it was shown that optimum

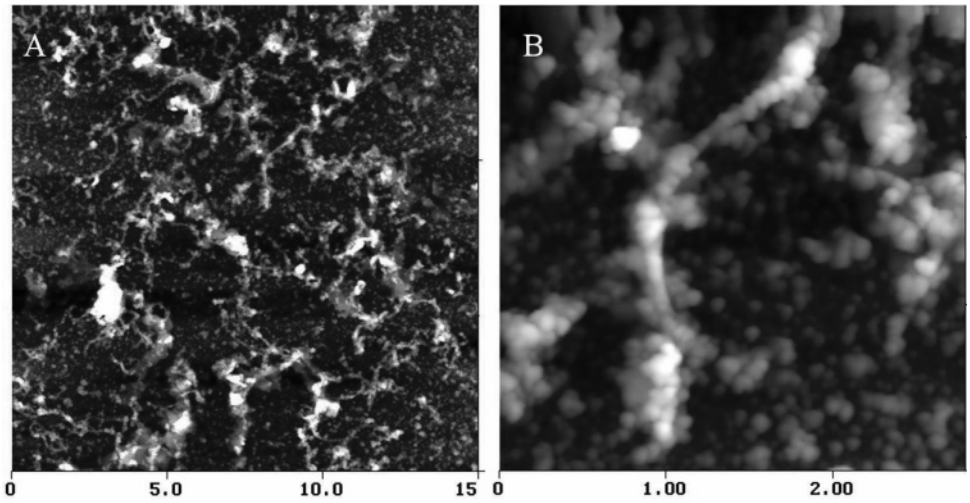

Figure 4. TM-AFM imaging on composite **1** drop-cast onto SiO_2 wafer and allowed to evaporate for 24 h. Image dimensions: (A) 15.0 × 15.0 μm^2, *z*-range = 200 nm and (B) 2.798 × 2.798 μm^2, *z*-range = 175 nm.

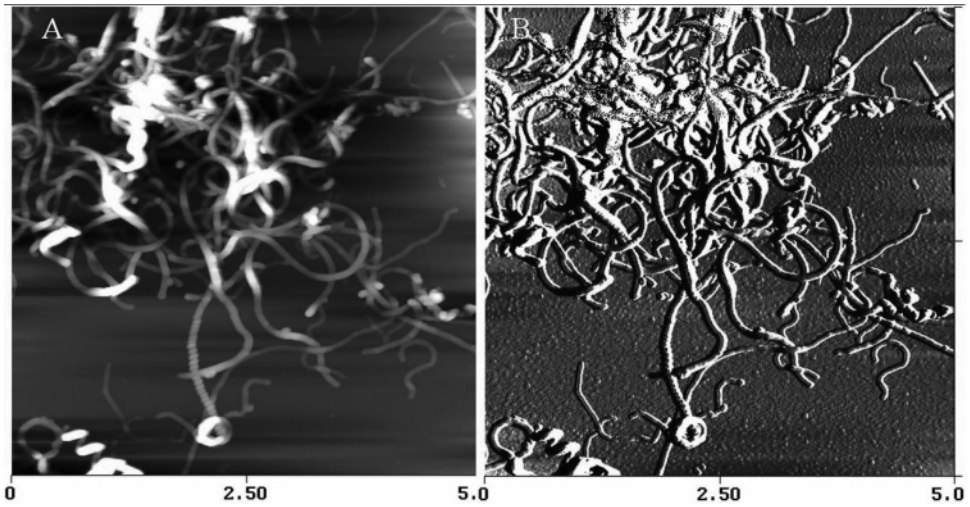

Figure 5. TM-AFM imaging on composite **1** drop-cast onto SiO_2 wafer after washing treatment. (A) AFM image with dimensions 5.0 × 5.0 μm^2 and *z*-range 175 nm and (B) corresponding amplitude data.

interaction with nanotubes can be linked to backbone exposure in the polymer. These polymers share an important characteristic, e.g., the presence of double bonds in the polymer backbone, which makes them ideal for noncovalent (attractive) interactions with the nanotube surface. This has generally been referred to as π-stacking of the polymer backbone on the nanotube surface. Changes in the optical spectroscopy can be directly linked to changes in the polymer conformation due to the presence of these double bonds. Double bonds are absent in the backbone of our metallopolymers and thus the attractive interaction will be different compared to that of conjugated polymers. Most important, functionalization of nanotubes with metallopolymers will not be facilitated by π-stacking of the polymer backbone (onto the nanotube surface), but by π-stacking of the ligands. One would expect that the π-system of (metallopolymers') ligands would facilitate a strong interaction with the nanotube surface and a significant effect on the MLCT transitions. However, as the MLCT transitions only reduce in intensity it is suggested that steric issues probably prevent a strong interaction (with nanotubes). This would suggest that the polymer conformation itself is not significantly affected. The spectroscopic data agree well with this suggestion as the most observable change is the reduction in intensity of MLCT transitions. Further theoretical work on the interaction between metallopolymers and carbon nanotubes and the morphology of metallopolymers absorbed onto the nanotubes' surface is necessary to fully understand the conformational changes in these metallopolymers (for examples of such investigations see refs 16, 41, and 42).

4. Conclusions

This work has shown that SWNT and MWNT can be stabilized in redox metallopolymers containing poly(pyridyl) complexes of ruthenium(II) and osmium(II). Microscopy (AFM and TEM) analysis has shown excellent wetting of the nanotubes with metallopolymers, thus demonstrating an attractive interaction between polymers and nanotubes. Spectroscopic analysis has shown that interactions with nanotubes do not significantly affect the metallopolymers' electrochemical properties. It is suggested that the resulting composite materials are likely to exhibit redox properties similar to that of free polymer. The interaction with nanotubes then adds functionality, as combining nanotubes and metallopolymers into composites could result in redox active materials with enhanced mechanical properties. The fact that in the polymer−nanotube assemblies the electrochemical and electronic properties of the polymers are maintained opens the possibility for their application of the assemblies as

nanosized electrochemical sensors for a range of both chemical and biological analytes, with the polymer coating acting as a redox catalyst. Further studies are currently in progress.

Acknowledgment. F.F., W.H., J.H. and J.G.V. would like to thank Enterprise Ireland for financial assistance. M.i.h.P. and N.A.Y. acknowledge support from EPSRC and The University of Hull. Mrs. J. Halder of the University of Hull Microscopy Facility is thanked for electron microscopy images.

Supporting Information Available: UV−vis absorption spectra of Ru- and Os-metallopolymers, Raman spectra of HiPco SWNT and **2**, and tapping mode AFM images of MWNT, **2**, **3**, and **4**. This material is available free of charge via the Internet at http://pubs.acs.org.

References and Notes

(1) Iijima, S. *Nature* **1991**, *354*, 58.

(2) Huang, W. Z.; Zhang, X. B.; Tu, J. P.; Kong, F. Z.; Ma, J. X.; Liu, F.; Lu, H. M.; Chen, C. P. *Mater. Chem. Phys.* **2002**, *78*, 144.

(3) Sun, Y.-P.; Zhou, B.; Henbest, K.; Fu, K.; Huang, W.; Lin, Y.; Taylor, S.; Carroll, D. L. *Chem. Phys. Lett.* **2002**, *351*, 349.

(4) Sander, S. J.; Tans, J.; Verschueren, A. R. M.; Dekker, C. *Nature* **1998**, *393*, 49.

(5) Chen, J.; Dyer, M. J.; Yu, M.-F. *J. Am. Chem. Soc.* **2001**, *123*, 6201.

(6) Chambers, G.; Carroll, C.; Farrell, G. F.; Dalton, A. B.; McNamara, M.; Cummins, E.; in het Panhuis, M.; Byrne, H. J. *Nano Lett.* **2003**, *3*, 843.

(7) O'Connell, M. J.; Bachilo, S. M.; Huffman, C. B.; Moore, V. C.; Strano, M. S.; Haroz, E. H.; Rialon, K. L.; Boul, P. J.; Noon, W. H.; Kittrell, C.; Ma, J.; Hauge, R. H.; Smalley, R. E. *Science* **2002**, *297*, 593.

(8) Richard, C.; Balavoine, F.; Schultz, P.; Ebbesen, T. W.; Mioskowski, C. *Science* **2003**, *300*, 775.

(9) Wenseleers, W.; Vlasov, I. I.; Goovaerts, E.; Obraztsova, E. D.; Lobach, A. S.; Bouwen, A. *Adv. Funct. Mater.* **2004**, *14*, 1105.

(10) Moore, V. C.; Strano, M. S.; Haroz, E. H.; Hauge, R. H.; Smalley, R. E.; Schmidt, J.; Yeshayahu, T. *Nano Lett.* **2003**, *3*, 1379.

(11) Hwang, G. L.; Hwang, K. C. *J. Mater. Chem.* **2001**, *11*, 1722.

(12) in het Panhuis, M.; Salvador-Morales, C.; Franklin, E.; Chambers, G.; Fonsca, A.; Nagy, J. B.; Blau, W. J.; Minett, A. I. *J. Nanosci. Nanotechnol.* **2003**, *3*, 209.

(13) Lin, Y.; Taylor, S.; Li, H.; Fernando, K. A. S.; Qu, L.; Wang, W.; Gu, L.; Zhou, B.; Sun, Y.-P. *J. Mater. Chem.* **2004**, *14*, 527.

(14) Ajayan, P. M.; Stephan, O.; Colliex, C.; Trauth, D. *Science* **1994**, *256*, 1212.

(15) McCarthy, B.; Coleman, J. N.; Czerw, R.; Dalton, A. B.; in het Panhuis, M.; Maiti, A.; Drury, A.; Byrne, H. J.; Carroll, D. L.; Blau, W. J. *J. Phys. Chem. B* **2002**, *106*, 2210.

(16) in het Panhuis, M.; Maiti, A.; Dalton, A. B.; van den Noort, A.; Coleman, J. N.; McCarthy, B.; Blau, W. J. *J. Phys. Chem. B* **2003**, *107*, 478.

(17) Rouse, J. H. *Langmuir* **2005**, *21*, 1055.

(18) Dalton, A. B.; Stephan, C.; Coleman, J. N.; McCarthy, B.; Ajayan, P. M.; Lefrant, S.; Bernier, P.; Blau, W. J.; Byrne, H. J. *J. Phys. Chem. B* **2000**, *104*, 10012.

(19) in het Panhuis, M.; Kane-Maguire, L. A. P.; Moulton, S. E.; Innis, P. C.; Wallace, G. G. *J. Nanosci. Nanotechnol.* **2004**, *4*, 976.

(20) Kymakis, E.; Amaratunga, G. A. J. *Synth. Met.* **2004**, *142*, 161.

(21) Chen, G. Z.; Shaffer, M. S. P.; Coleby, D.; Dixon, G.; Zhou, W. Z.; Fray, D. J. *Adv. Mater.* **2000**, *7*, 522.

(22) Maser, W. K.; Benito, A. M.; Callejas, M. A.; Seeger, T.; Martinez, M. T.; Schreiber, J.; Muszynski, J.; Chauvet, O.; Osvath, Z.; Koos, A. A.; Biro, L. P. *Mater. Sci. Eng. C* **2003**, *23*, 87.

(23) Keogh, S. M.; Hedderman, T. G.; Rüther, M. G.; Lyng, F. M.; Gregan, E.; Farrell, G. F.; Chambers, G.; Byrne, H. J. *J. Phys. Chem. B* **2005**, *109*, 5600.

(24) Ryan, K. P.; Lipson, S.; Drury, A.; Cadek, M.; Ruether, M.; O'Flaherty, S. M.; Barrow, V.; McCarthy, B.; Byrne, H. J.; Blau, W. J.; Coleman, J. N. *Chem. Phys. Lett.* **2004**, *391*, 329.

(25) Sainz, R.; Benito, A. M.; Teresa Martinez, M.; Galindo, J. F.; Sotres, J.; Baro, A. M.; Corraze, B.; Chauvet, O.; Maser, W. K. *Adv. Mater.* **2005**, *17*, 278.

(26) in het Panhuis, M.; Thielemans, W.; Minett, A. I.; Leahy, R.; Le Foulgoc, B.; Blau, W. J.; Wool, R. P. *Int. J. Nanosci.* **2003**, *2*, 185.

(27) Marder, S. R.; Perry, J. W. *Proceedings of the SPIE*: *Organic, Metallorganic, and Polymeric Materials for Non-Linear Optical Applications*; *SPIE*: Los Angles, CA, 1994.

(28) Forster, R. J.; Vos, J. G. *Electrochim. Acta* **1992**, *37*, 159.

(29) Hogan, C. F.; Forster, R. J. *Anal. Chim. Acta* **1999**, *396*, 13.

(30) Forster, R. J.; Figgemeir, E.; Lees, A. C.; Hjelm, J.; Vos, J. G. *Langmuir* **2000**, *16*, 7867.

(31) Doherty, A. P.; Forster, R. J.; Smyth, M. R.; Vos, J. G. *Anal. Chim. Acta* **1991**, *255*, 45.

(32) Doherty, A. P.; Forster, R. J.; Smyth, M. R.; Vos, J. G. *Anal. Chem.* **1992**, *64*, 572.

(33) Doherty, A. P.; Vos, J. G. *J. Chem. Soc., Faraday Trans.* **1992**, *88*, 2903.

(34) Doherty, A. P.; Stanley, M. A.; Vos, J. G. *Analyst* **1995**, *120*, 2371.

(35) Rajaopolan, C. R.; Aoki, A.; Heller, A. *J. Phys. Chem.* **1996**, *100*, 3719.

(36) Forster, R. J.; Vos, J. G. *Macromolecules* **1990**, *23*, 4372.

(37) Nikolaev, P.; Bronikowski, M.; Bradley, R.; Roymund, F.; Colbert, D.; Smith, K.; Smalley, R. *Chem. Phys. Lett.* **1999**, *313*, 91.

(38) Geraty, S. M.; Vos, J. G. *J. Chem. Soc., Dalton Trans.* **1987**, 3073.

(39) Chen, G.; Sumanaskera, G. U.; Pradhan, B. K.; Gupta, R.; Eklund, P. C.; Bronikowski, M. J.; Smalley, R. E. *J. Nanosci. Nanotechnol.* **2002**, *2*, 621.

(40) in het Panhuis, M.; Munn, R. W.; Blau, W. J. *Synth. Met.* **2001**, *121*, 1187.

(41) Grujicic, M.; Gao, G.; Roy, W. N. *Appl. Surf. Sci.* **2004**, *227*, 349.

(42) Yang, M.; Koutos, V.; Zaiser, M. *J. Phys. Chem. B* **2005**, *109*, 10009.